Spiky phases of smooth membranes. Implications for smooth strings

H. Kleinert[a]

Freie Universität Berlin, Institut für Theoretische Physik, Arnimallee 14, 14195 Berlin, Germany

Abstract. We point out a possible mechanism by which smooth surfaces can become spiky as the constant of curvature stiffness κ falls below a certain critical value. This happens either in a single first-order transition, or in a sequence of two Kosterlitz-Thouless-like transitions. There may also be additional phases in which the spikes form a hexagonal solid-like array or a disordered liquid-like structure. Our discussion suggests that there exist smooth strings between quarks.

PACS. 68.35.Rh Phase transitions and critical phenomena – 68.35.Wm Other nonelectronic properties

1 Introduction

We would like to point out a possible rather universal mechanism by which spiky superstructures can form on a membrane. These can undergo several interesting phase transitions, whose nature we predict.

The existence of superstructures on membranes has been investigated by many authors, in particular wormhole [1] and egg-carton shapes [2,3]. There are also experimental indications [4] that such structures exist. An example is shown in Figure 1, although it is by no means clear that this particular state can be explained by the phase transitions to be described in this note.

Consider closed amphiphilic vesicles dispersed in water, forming in general smooth tensionless surfaces [5] whose effective energy is governed by curvature stiffness [6]:

$$E = \frac{1}{2} \int \mathrm{d}^2 x \sqrt{g} \left[\kappa_0 (c_1 + c_2)^2 + \bar{\kappa}_0 c_1 c_2 \right], \qquad (1)$$

where κ_0 is of the order of eV. Here $(c_1 + c_2)/2$ and $c_1 c_2$ denote the mean and the Gaussian curvature, respectively, $x = (x^1, x^2)$ are arbitrary parameters of the surface, and $g_{ij}(x)$ is the intrinsic metric. This energy is certainly only an approximation, valid for small curvatures. If the curvatures increase, there will be deviations from this simple quadratic behavior. Moreover, since membranes are composed of rod-like molecules of a certain length r_0, there exists a natural maximal curvature $c_1 = c_2 = 1/r_0$ beyond which a membrane cannot be bent without destroying the microscopic structure. Between zero and this maximal value, the increase in energy will slow down. This property is caused by various important contributions to

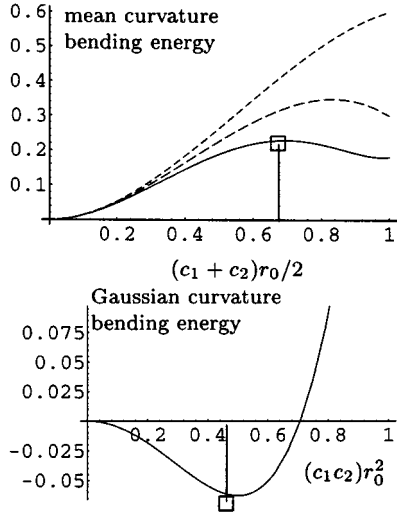[a] e-mail: `kleinert@physik.fu-berlin.de`
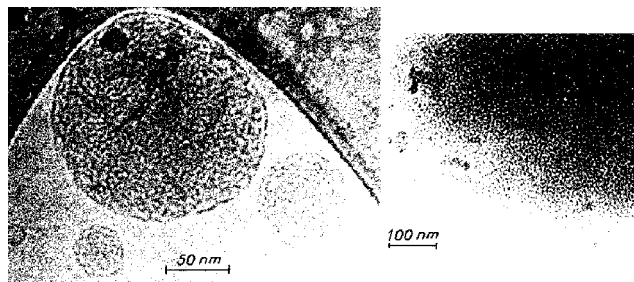
Fig. 1. Rough surface structure observed by Kloesgen and Helfrich [4] in dioleoylphosphatidylcholine (DOPC) bilayers.

the bending stiffness [3,7]. As a function of the mean curvature, the bending energy of many membranes may have a maximum at a certain value c_m of $(c_1 + c_2)/2$, as sketched in Figure 2. Such a maximum supplies the system with a second characteristic length scale $r_m = 1/c_m$ at which interesting new phenomena should be observed. A further length scale arises from higher powers of the Gaussian curvature in the energy density. Assuming, for example, the presence of terms $\kappa_2 (c_1 c_2)^2 + \kappa_4 (c_1 c_2)^4$, with coefficients $\kappa_2 \approx -1$ eV Å^2, $\kappa_4 \approx 1$ eV (30 Å)^8, Monte-Carlo simulations [8] have shown the existence of a periodic egg carton superstructure with a period of the order of $r_m = 60$ Å.

Membranes with an additional length scale of either type will be the objects of study in this note. Certainly, the energy of a single spike will be quite large (maybe of the order of $10 k_B T$) so that their Boltzmann factor is quite small. We shall see, however, that configuration entropy can compensate this large energy at high enough temperatures.

Fig. 2. Possible behaviors of bending energy as a function of mean curvature $(c_1 + c_2)/2$ measured in units of the inverse molecular size r_0.

2 Reminder of fluctuation properties of membranes

Before we come to our actual theory, let us first recall some well-known properties of membrane fluctuations governed only by the energy (1), with a partition function (in natural units where the Boltzmann constant is equal to 1)

$$Z = \sum_{\text{conf}} e^{-E/T}, \qquad (2)$$

where $\sum_{\text{conf}}$ denotes a sum over all membrane configurations. As a consequence of the anharmonic nature of the energy (1) when expressed in terms of the positions of the membrane molecules, thermal fluctuations make the first coupling constant, the *extrinsic curvature stiffness*, *soften* with temperature as [9,10]

$$\kappa = \kappa_0 - 3(T/8\pi) \log\left(r_{\text{IR}}^2/r_{\text{UV}}^2\right). \qquad (3)$$

Here r_{UV} is a short-distance (UV) cutoff equal to the size of the molecules r_0, whereas r_{IR} is a long-distance (IR) cutoff set by the size of a vesicle. The small parameter in the perturbation expansion leading to (3) is the inverse stiffness $1/\kappa$, the *flexibility*. The result (3) is obtained from an infinite bubble sum of diagrams, which is equivalent to a Hartree-Fock-Bogoliubov approximation [10]. That approximation gives usually a good idea for what happens also for large flexibilities, *i.e.* small κ. If we trust equation (3) in this regime, we conclude that the extrinsic curvature vanishes for large vesicles, whose size exceed the so-called *persistence length* [11]

$$\xi = r_{\text{UV}} e^{4\pi\kappa_0/3T}. \qquad (4)$$

On the basis of this, we may expect vesicles of a size much larger than ξ to look crumpled. This has indeed been confirmed in computer simulations [12].

For the second coupling constant $\bar{\kappa}_0$ in (1), the *Gaussian curvature stiffness*, this effect is absent since this constant *hardens* as follows [13]

$$\bar{\kappa} = \bar{\kappa}_0 + (10/3)(T/8\pi) \log\left(r_{\text{IR}}^2/r_{\text{UV}}^2\right). \qquad (5)$$

An important question is whether the persistence length (4) reflects a true property of the theory, or is merely a consequence of the Hartree-Fock-Bogoliubov approximation which will not survive higher-loop corrections.

In an attempt to answer this question, consider a single surface fluctuating around an infinitely large planar configuration in d dimensions with periodic boundary conditions. This surface may be described by a vector field $X^\mu(x)$ $(d = 1, \ldots, d)$, giving rise to the intrinsic metric $g_{ij}(x) = \partial_i X^\mu(x) \partial_j X_\mu(x)$ where $(i, j = 1, 2)$. The contraction of the spatial vector indices μ is performed *via* the Euclidean unit matrix $G_{\mu\nu} = \delta_{\mu\nu}$. In terms of $X^\mu(x)$, the energy (1) can be written more explicitly as

$$E = \frac{1}{2} \int d^2x \sqrt{g(x)} [\kappa_0 D^2 X^\mu(x) D^2 X_\mu(x)$$
$$+ \bar{\kappa}_0 (D^2 X^\mu D^2 X_\mu - D_\nu D_\lambda X^\mu D^\nu D^\lambda X_\mu)], \qquad (6)$$

where D_μ is the covariant derivative formed with the help of the Christoffel symbol $\Gamma_{ij}{}^k = g^{kl}(\partial_i g_{jl} + \partial_j g_{il} - \partial_l g_{ij})/2$. The Gaussian curvature energy can be ignored, since it is a constant depending only on the genus of the surface which assume to remain invariant.

We shall choose a special parametrization due to Monge, in which $X^1(x) = x^1$, $X^2(x) = x^2$, and $X^{a+2}(x) = u^a(x)$ with $(a = 1, \ldots, d-2)$, so that $g_{ij}(x) = \delta_{ij} + \partial_i u_a(x) \partial_j u^a(x)$, with the contraction over indices a being performed via the $(d-2) \times (d-2)$-dimensional submatrix δ_{ab} of $G_{\mu\nu}$. Then we rewrite the energy (6) in yet another form as [14]

$$E' = \frac{\kappa_0}{2} \int d^2x \sqrt{h} [D^2 X^a D^2 X_a$$
$$+ \lambda^{ij}(\partial_i X^a \partial_j X_a + \delta_{ij} - h_{ij})], \qquad (7)$$

where $h_{ij}(x)$ and $\lambda_{ij}(x)$ are two auxiliary symmetric fields. The partition function of the surface is then given by the functional integral

$$Z = \int \mathcal{D}u \mathcal{D}\lambda_{ij} \mathcal{D}h_{ij} e^{-E'/T}. \qquad (8)$$

The integral over $\lambda_{ij}(x)$ ensures that the auxiliary field $h_{ij}(x)$ coincides with the induced metric $g_{ij}(x)$, and thus the equality of Z with the partition function $Z = \int \mathcal{D}X e^{-E/T}$ for the original energy (6) [or (1)], if the parametrization is fixed likewise. In the sequel we shall measure the stiffness constants in units of temperature so that we can set $T = 1$ everywhere.

The advantage of the functional integral (7) is that the surface positions $u^a(x)$ can be integrated out, leaving a purely intrinsic effective energy

$$E^{\text{eff}} = \frac{d-2}{2} \Big\{ \text{Tr} \log[(D^2)^2 - D_i \lambda^{ij} D_j]$$
$$- \frac{\kappa_0}{d-2} \int d^2x \sqrt{g} \lambda^{ij} h_{ij} \Big\}. \qquad (9)$$

In the limit $d \to \infty$, the fluctuations of the fields $\lambda^{ij}(x), h_{ij}(x)$ are frozen, and the energy is given by the saddle point approximation. For symmetry reasons, the saddle point has constant diagonal fields $h_{ij} = \rho\,\delta_{ij}$, $\lambda^{ij} = \lambda h^{ij} = (\lambda/\rho)\delta_{ij}$, so that the energy reads

$$E = \frac{d-2}{2}\Delta x^1 \Delta x^2 \rho \left\{ \left[\int \frac{\mathrm{d}^2 k}{(2\pi)^2} \log(k^4 + \lambda k^2) \right. \right.$$
$$\left. \left. -2\frac{\kappa_0}{d-2}\lambda \right] + 2\frac{\kappa_0}{d-2}\frac{\lambda}{\rho} \right\}, \tag{10}$$

to be extremized in ρ and λ. Here $\Delta x^1 \Delta x^2$ is the base area of the surface. Performing the integral with a momentum space cutoff Λ of the order of the inverse molecular size r_{UV} we find

$$\int_{|k|<\Lambda} \frac{\mathrm{d}^2 k}{(2\pi)^2} \log(k^2 + \lambda) = \frac{1}{4\pi}[(\Lambda^2 + \lambda)\log(\Lambda^2 + \lambda)$$
$$- \Lambda^2 - \lambda\log\lambda]$$
$$= \frac{1}{4\pi}[\Lambda^2(\log\Lambda^2 - 1) + (\log\Lambda^2 + 1)\lambda - \lambda\log\lambda]$$
$$+ \mathcal{O}(1/\Lambda^2), \tag{11}$$

and the brackets in (10) become

$$\frac{1}{4\pi}[2\Lambda^2(\log\Lambda^2 - 1) + (\log\Lambda^2 + 1)\lambda - \lambda\log\lambda] - 2\frac{\kappa_0}{d-2}\lambda. \tag{12}$$

The first constant term can be absorbed into the measure of the functional integral (8). The logarithmic divergence multiplying λ may be removed by introducing a renormalized stiffness

$$\kappa = \kappa_0 - \frac{d-2}{8\pi}\left(\log\frac{\Lambda^2}{\mu^2} + 1\right) \tag{13}$$

where μ is some mass scale, on which κ depends [$\kappa = \kappa(\mu)$]. For μ equal to the inverse of the molecular size r_{UV}, we have $\kappa(r_{\mathrm{UV}}^{-1}) = \kappa_0$. With the help of κ, the bracket in (10) becomes

$$-\frac{1}{4\pi}\lambda\log\frac{\Lambda^2}{\mu^2} - 2\frac{\kappa}{d-2}\lambda. \tag{14}$$

Introducing further a μ-independent mass scale (the so-called *dimensionally transmuted coupling constant*)

$$\bar\lambda = \mu^2 e^{-[2/(d-2)]4\pi\kappa(\mu)+1}, \tag{15}$$

expression (12) takes a μ- and cutoff-independent form

$$-\frac{1}{4\pi}\lambda\log\frac{\lambda}{\bar\lambda}, \tag{16}$$

and the energy (10) can be rewritten as

$$E = \frac{d-2}{2}\Delta x^1 \Delta x^2 \rho\left(f_0 - \frac{\lambda}{4\pi} + \kappa\frac{\lambda}{\rho}\right),$$
$$f_0 \equiv -\frac{\lambda}{4\pi}\left(\log\frac{\lambda}{\bar\lambda} - 1\right). \tag{17}$$

A multiplicative renormalization constant $Z_\kappa = \kappa_0/\kappa$ has been absorbed into λ and $\bar\lambda$, so that all quantities are now finite for $\Lambda \to \infty$.

Extremizing (17) in ρ yields $f_0 = \lambda/4\pi$ and thus $\lambda = \bar\lambda$, where $f_0 - \lambda/4\pi = 0$. Extremizing (17) in λ yields $\kappa/\rho = 1/4\pi$, so that the extremal energy (17) is

$$E^{\mathrm{ext}} = \frac{d-2}{2}\Delta x^1 \Delta x^2 \frac{\bar\lambda}{4\pi}. \tag{18}$$

From the trace of the logarithm in (9) we see that $\bar\lambda$ sets a mass scale for the correlation function $\langle D_i u^a D_j u^b \rangle$ which falls off like $e^{-|x|\sqrt{\bar\lambda}}$ for large $|x|$, showing that $1/\sqrt{\bar\lambda}$ plays the role of the persistence length (4). Thus the $d \to \infty$ model possesses precisely the properties which we derived for a real membrane in three dimensions by a Hartree-Fock-Bogoliubov approximation.

The question of corrections to this approximation is therefore equivalent to the problem of lowering d down to the physical dimension 3. Since we are unable to treat the model for finite d, let us gain insight into its possible properties by comparing it to an analogous very similar model, which is also exactly solvable for a parameter $N \to \infty$, which plays the same role as $d-2$ in the above discussion. This is the $O(N)$ nonlinear σ-model for which the case $N = 2$ is well-known to have quite different properties from those derived from the $N \to \infty$-limit. This knowledge will shed some light upon the behavior of surfaces for small $d-2$.

3 Relevant properties of O(N)-symmetric nonlinear σ-models

The $O(N)$-symmetric nonlinear σ-model consists of a fluctuating field of unit vectors with N components

$$n_a(x)\,(a = 1, \ldots, N),\, n_a^2(x) = 1, \tag{19}$$

in a two-dimensional x-space, with a partition function given by the functional integral

$$Z_\sigma = \prod_x \left[\int \frac{\mathrm{d}^{N-1}n_a}{S_N} \right] \exp\left[-\frac{\kappa_0}{2}\int \mathrm{d}^2 x(\partial n^a)^2 \right], \tag{20}$$

where $S_N \equiv 2\pi^{N/2}/\Gamma(N/2)$ is the surface of a sphere in N dimensions covered by the directional integral $\mathrm{d}^{N-1}n^a$, so that $\int \mathrm{d}^{N-1}n^a/S_N = 1$. Just as the surface model for $d \to \infty$, this model is exactly solvable in the limit $N \to \infty$, where it is referred to as the *spherical model*, first solved by Berlin and Kac in 1952 [15]. As in the energy (7), we introduce an auxiliary field $\lambda(x)$ and rewrite (20) as

$$Z_\sigma = \int \mathcal{D}^N n_a \int_{-i\infty}^{i\infty} \mathcal{D}\lambda \exp\left\{ -\frac{\kappa_0}{2}\int \mathrm{d}^2 x \left[(\partial n_a)^2 \right. \right.$$
$$\left. \left. + N\lambda(n_a^2 - 1) \right] \right\}, \tag{21}$$

where the λ-integrations run from $-i\infty$ to $i\infty$. Now the n_a-integrals are Gaussian and can be done, leading to

$$Z_\sigma = \int_{-i\infty}^{i\infty} \mathcal{D}\lambda \exp\left\{-\frac{N}{2}\left[\mathrm{Tr}\log(-\partial^2+\lambda)+\kappa_0\int \mathrm{d}^2x\lambda(x)\right]\right\}. \tag{22}$$

In the limit $N \to \infty$, the λ-fluctuations are frozen at the saddle point, which lies at a constant $\lambda(x) \equiv \lambda$, and has an energy

$$E_\sigma = \frac{N}{2}\Delta x^1 \Delta x^2 \left[\int \frac{\mathrm{d}^2k}{(2\pi)^2}\log(k^2+\lambda)-\frac{\kappa_0}{N}\lambda\right]. \tag{23}$$

Regularizing the integral as before, this becomes

$$E = \frac{N}{2}\Delta x^1 \Delta x^2 \rho f_0, \quad f_0 \equiv -\frac{\lambda}{4\pi}\left(\log\frac{\lambda}{\bar\lambda}-1\right), \tag{24}$$

where $\bar\lambda = \mu^2 \exp\{-4\pi\kappa(\mu)/N\}$ is the dimensionally transmuted coupling constant of the σ-model. It gives a nonzero length scale $1/\sqrt{\bar\lambda}$ to the fluctuations of the vector field n_a which have a correlation function $\propto \mathrm{e}^{-|x|\sqrt{\bar\lambda}}$.

The similarity of the two models is quite obvious. The advantage of the latter is that it is well understood. Since the work of Kosterlitz and Thouless in 1973 [16] it is known that $N \to \infty$ properties are found in the model only down to $N = 3$ (classical Heisenberg model). For $N = 2$, the model possesses at large $\kappa_0 \geq \kappa_0^c = 2/\pi$ an extra phase in which the correlation functions of the vector field n_a have a long range, falling off algebraically like $1/|x|^{\mathrm{const}}$ rather than exponentially. This is most easily seen by parametrizing the two-component vector field N_a in terms of an azimuthal angle θ as $(N_a) = (\cos\theta, \sin\theta)$, and rewriting (20) as a functional integral

$$\tilde Z_\sigma = \sum_L \prod_x \left[\int \frac{\mathrm{d}\theta(x)}{2\pi}\right]$$
$$\times \exp\left\{-\frac{\kappa_0}{2}\int \mathrm{d}^2x[\partial_i\theta(x)-2\pi\delta_i(x;L)]^2\right\}, \tag{25}$$

where $\delta_i(x;L) \equiv \epsilon_{ij}\int \mathrm{d}\xi_j\delta^{(2)}(x-\bar x(\xi))$ is the δ-function on a line L described by $\bar x(\xi)$, pointing orthogonal to the line elements. The sum $\sum_L$ runs over a grand-canonical ensemble of lines L. The sum is necessary to preserve the cyclic invariance of the energy in (20) under cyclic replacements $\theta(x) \to \theta(x) + 2\pi\delta(x;S)$, where $\delta(x;S) \equiv \int \mathrm{d}^2\xi\delta^{(2)}(x-\bar x(\xi))$ is the δ-function on the surface S described by $\bar x(\xi)$ [17]. The energy in (25) is a direct consequence of the identity $\partial_i e^{i\theta(x)} = e^{i\theta(x)}[\partial_i\theta(x)-2\pi\delta_i(x;L)]$.

We may now introduce an auxiliary field $b_i(x)$ and rewrite $\tilde Z_\sigma$ as

$$\tilde Z_\sigma = \sum_L \prod_x \left[\int \frac{\mathrm{d}\theta(x)}{2\pi}\int \mathrm{d}b_i\right]$$
$$\times \exp\left\{\kappa_0\int \mathrm{d}^2x\left(\frac{b_i^2(x)}{2}-i\,b_i(x)[\partial_i\theta(x)-2\pi\delta_i(x;L)]\right)\right\}. \tag{26}$$

The integrals over $\theta(x)$ can now be performed, which gives the condition that the field b_i must be divergenceless [17]. This may be enforced by setting $b_i = \epsilon_{ij}\partial_j u$, and the partition function (26) becomes

$$\tilde Z_\sigma = \sum_{\{x_i,x_f\}} \prod_x \left[\int \mathrm{d}u(x)\right]$$
$$\times \exp\left\{\kappa_0\int \mathrm{d}^2x\left[\frac{1}{2}[\partial_i u(x)]^2 - 2\pi i u(x)n(x)\right]\right\}, \tag{27}$$

where

$$n(x) = \epsilon_{ij}\partial_i\delta_j(x;L) = \delta^{(2)}(x-x_i) - \delta^{(2)}(x-x_f) \tag{28}$$

is the density of initial and final end points of the line L, which lie at x_i and x_f, respectively, with positive and negative signs. These are the positions of vortices and antivortices in the original field configurations $\theta(x)$. By integrating out the u-field in (27), we obtain

$$\tilde Z_\sigma = \sum_{\{x_i,x_f\}} \exp\left[-\frac{\kappa_0}{2}4\pi^2\right.$$
$$\left.\times \int \mathrm{d}^2x\int \mathrm{d}^2x'n(x)G(x-x')n(x')\right], \tag{29}$$

where

$$G(x-x') = \int \frac{\mathrm{d}^2k}{(2\pi)^2}\frac{\mathrm{e}^{ikx}}{k^2} = -\frac{1}{2\pi}\log\frac{|x-x'|}{r_0} + \log\frac{r_{\mathrm{IR}}}{r_0^2} \tag{30}$$

is the correlation function of the field $u(x)$ containing some finite length scale r_0 and an infrared cutoff r_{IR} which goes to infinity. However, this infinity drops out in the partition function (29) since $\int \mathrm{d}^2x\,n(x) = 0$ due to the equal number of initial and final endpoints x_i, x_f in the sum over all initial and final points Σ_{x_i,x_f} of the lines L in the grand-canonical ensemble.

Let us derive the partition function (29) in a slightly different, more phenomenological way which will be useful to understand the spiky membranes. Suppose we are given the partition function (27) without vortices, where the energy is simply

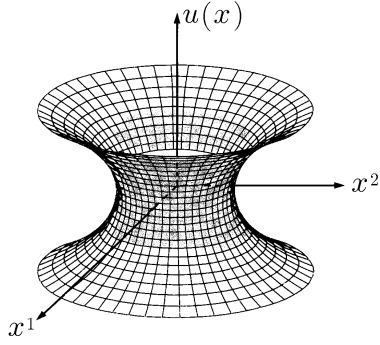$$\tilde E_\sigma^{\mathrm{lin}} = \frac{\kappa_0}{2}\int \mathrm{d}^2x(\partial_i u)^2. \tag{31}$$

The equation of motion

$$\partial^2 u(x) = 0 \tag{32}$$
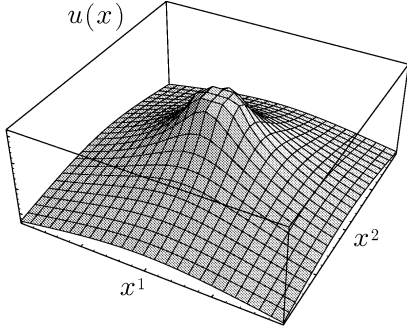
has two types of rotationally invariant solutions. The trivial $u(x) \equiv 0$, and the solution

$$u_{\mathrm{wh}}(x) = \mp A\frac{1}{2\pi}\log\frac{r}{r_0}, \quad r > r_0, \quad r \equiv |x|, \tag{33}$$

which satisfies $-\partial^2 u_{\mathrm{wh}} = 0$. The amplitude A is arbitrary. If we interpret $u(x)$ as a vertical displacement of a flat

Fig. 3. Wormhole solution of differential equation $\partial^2 u(x) = 0$.

Fig. 4. Spike-like solution of differential equation $\partial^2 u(x) = 0$, obtained from the lower branch of the "wormhole" solution in Figure 3 after capping it at the molecular scale r_{UV}.

surface in three dimensions, this looks like a "wormhole" in a curved planar space, as pictured in Figure 3.

This solution exists for any r_0. Let us now imagine the surface to consist of molecules of size r_{UV}. Then the smallest possible r_0 is r_{UV}. For this value, however, the throat of the wormhole can be closed by a small cap from above or below, thus becoming a spike-like surface shown in Figure 4 to be denoted by $u_{\mathrm{sp}}(x)$, or an antispike-like surface pointing downwards.

The linearized energy (32) of these surfaces is large so that only a few spikes and antispikes are present in thermal equilibrium. If a single spike-antispike pair with opposite orientation centered at different places x and y is inserted into the field energy (31), we obtain precisely the interaction energy of a vortex pair in the partition function (29) if we set $A = 1$. The size of A is a consequence of the vortex quantization in the original energy in (25). A spike and an antispike can combine to a dipole, and two of these to a quadrupole, as shown in Figure 5. In principle, there can also be a crystal-like array of spikes and antispikes, also shown in Figure 5. This requires the presence off additional higher-gradient terms in the energy (32) which would modify the short-distance properties appropriately [17].

The partition function (29) describes a neutral Coulomb gas. This is known to have a pair unbinding transition which is of infinite order at low temperatures, the Kosterlitz-Thouless transition. The transition point is easily calculated if only very few charges are present. At low temperatures, a single pair has an average square distance

$$\langle r^2 \rangle \propto \int_{r_0}^{\infty} \mathrm{d}r\, r\, \mathrm{e}^{-\kappa_0\, 2\pi \log(r/r_0)} r^2 \propto \frac{1}{4 - \kappa_0\, 2\pi}\, . \quad (34)$$

As the stiffness constant κ_0 falls below $\kappa_0^{\mathrm{c}} = 2/\pi$, the square distance diverges, and the electron gas enters a plasma phase in which the field $u(x)$ acquires a finite range, the *Debye* screening length r_{Debye}, which is precisely the inverse of $\sqrt{\lambda}$ in equation (24).

This result implies that the average value of $\lambda(x)$ which is calculated from the functional integral (22) as

$$\langle \lambda(x) \rangle = Z^{-1} \int_{-i\infty}^{i\infty} \mathcal{D}\lambda\, \lambda(x)$$
$$\times \exp\left\{ -\frac{N}{2}\left[\mathrm{Tr}\log(-\partial^2 + \lambda) + \kappa_0 \int \mathrm{d}^2 x\, \lambda(x) \right] \right\}, \quad (35)$$

and which has the nonzero average value $\langle \lambda(x) \rangle = \bar{\lambda}$ for small stiffness, vanishes for $N = 2$ and $\kappa_0 > \kappa_0^{\mathrm{c}}$. There the fluctuations of $\lambda(x)$ become so strong that the nonzero saddle point at $\lambda \equiv \bar{\lambda}$ looses control over the functional integral. The $\lambda(x)$-field acquire more and more zeros until, at a small enough N and large enough stiffness, these zeros proliferate making $\langle \lambda(x) \rangle = 0$. Up to now, nobody has been able to derive this result from the functional integral (35), but the above Coulomb gas argument proves that this must be true.

For a dilute gas of vortices, *i.e.*, for a high activation energy E_{v} and a small fugacity $z = \mathrm{e}^{-E_{\mathrm{v}}/T}$ of a vortex, the sum over all vortices and antivortices in the partition function (27) can be restricted to a single vortex or antivortex at each point, in which case the partition function goes over into

$$\tilde{Z}_\sigma \approx \prod_x \left[\int \mathrm{d}u(x) \right]$$
$$\times \exp\left\{ -\kappa_0 \int \mathrm{d}^2 x \left[\frac{1}{2}[\partial_i u(x)]^2 - \frac{z}{\kappa_0}\cos[2\pi\kappa_0 u(x)] \right] \right\}. \quad (36)$$

This is the partition function of the sine-Gordon model, which is thus equivalent to the $O(2)$ nonlinear σ-model. For small stiffness κ_0, we may expand $\cos[2\pi\kappa_0 u(x)] \approx 1 - 4\pi^2\kappa_0^2 u^2(x)/2$ to see that the fluctuations have a a finite range. For large stiffness $\kappa_0 > \kappa_0^{\mathrm{c}} = 2/\pi$, however, the cosine oscillates so rapidly that it no longer contributes to the functional integral. In this regime, the system has only long-range fluctuations [18].

4 Consequences for membranes

What are the lessons of all this for membrane fluctuations? Suppose we restrict the field fluctuations in (7) to diagonal fields $h_{ij}(x) = \rho(x)\delta_{ij}$ and $\lambda^{ij} = \lambda(x)h^{ij}(x)$ with the constant extremal $\rho = 4\pi\kappa$. Then we remain with
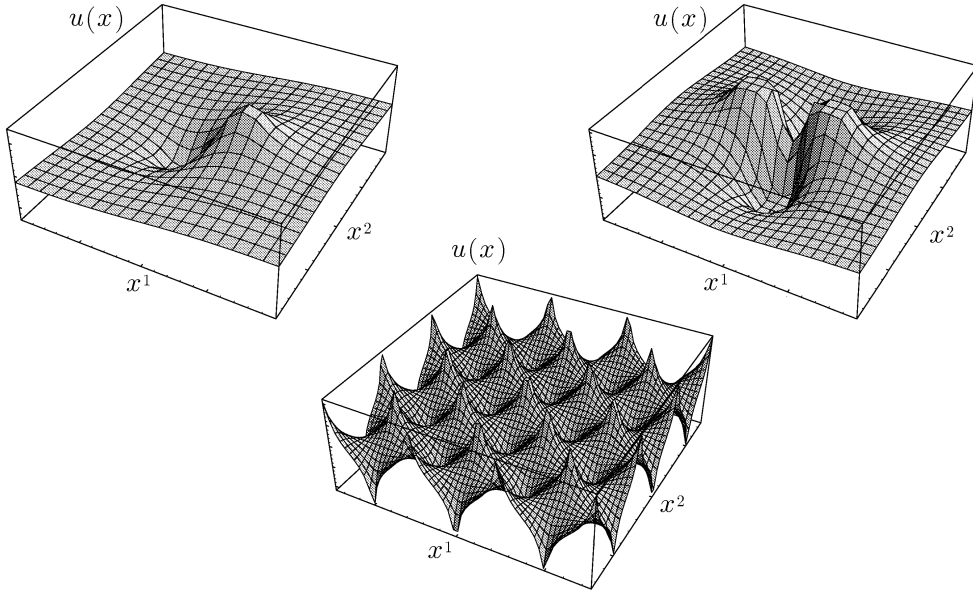
Fig. 5. Pair of spikes, quadrupole-, and crystal-like multipole solutions, obtained from a superposition of spike and antispike solutions of the differential equation $\partial^2 u(x) = 0$ in Figure 4.

a functional integral over $\lambda(x)$ with a Boltzmann factor $e^{-E'^{\text{eff}}/T}$ where E'^{eff} is the obvious generalization of the effective energy (9) to a functional of a space-dependent $\lambda(x)$, which has precisely the same form as functional the exponent in (22). But such a functional integral has just been shown to yield for a large enough stiffness κ a vanishing average $\langle \lambda(x) \rangle$, implying that the fluctuations of the derivatives $\partial_i u^a$ have an infinite range characteristic for a smooth surface. It is certainly suggestive that the additional neglected fluctuations in the energy (9), non-diagonal in $\lambda^{ij}(x)$ and arbitrary local in $h_{ij}(x)$ do not change this result.

How can we see whether this is true? Consider a linearized version of the energy (6)

$$\tilde{E}^{\text{lin}} = \frac{\kappa_0}{2} \int \mathrm{d}^2 x [\partial^2 u(x)]^2, \tag{37}$$

and let us go through the same argument as in the discussion of the linearized energy (31). The equation of motion

$$\partial^4 u(x) = 0 \tag{38}$$

has three types of solutions. First, there is the trivial one $u(x) \equiv 0$. Second, there are spike-like solutions $u_{\text{sp}}(x)$ arising from capping a wormhole solution (33) of the previous system, as shown in Figure 3. Third, and most importantly, there are spike-like solutions of the form

$$u_{\text{sp2}}(x) = \pm A \frac{\sqrt{3}}{2} \frac{1}{8\pi} \left[r^2 \log \frac{r}{r_0 e} - \frac{1}{2} \log \frac{r}{r_0 e^{1/6}} \right], \ r \equiv |x|, \tag{39}$$

which satisfy $-\partial^2 u_{\text{sp2}}(x) = u_{\text{sp}}(x)$ and $\partial^4 u_{\text{sp2}}(x) = \pm A \delta^{(2)}(x)$. With a cap of molecular size they have the form shown in Figure 6. There are also dipole, quadrupole, and multipole solutions displayed in Figure 7.
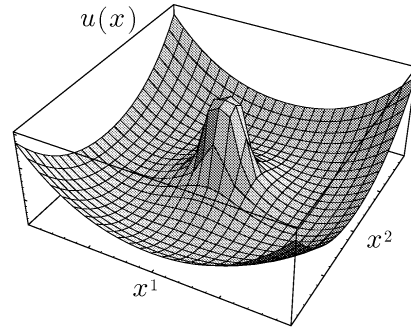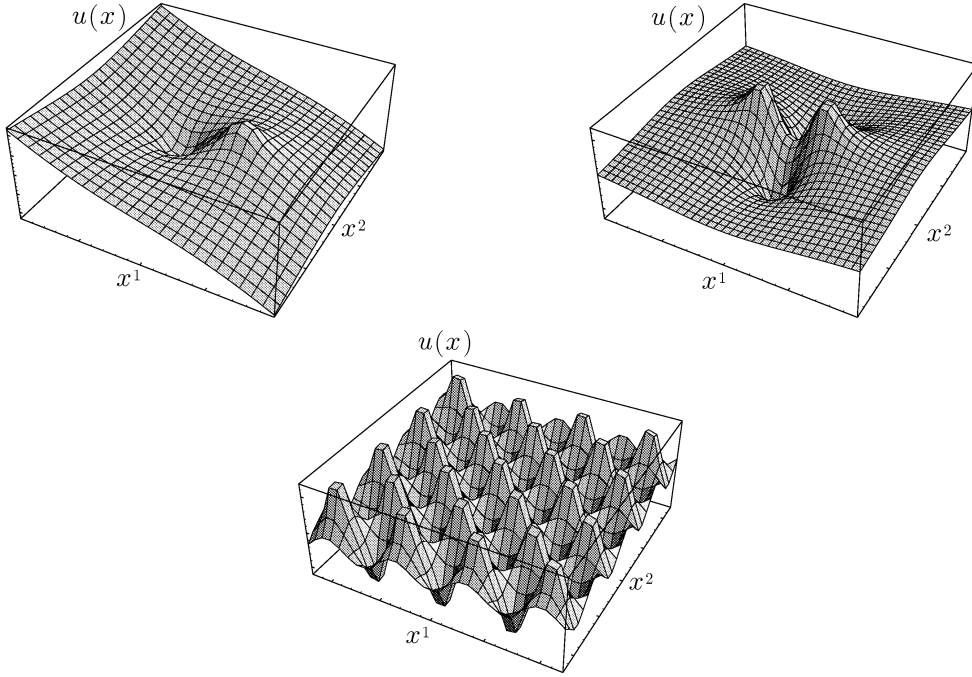

Fig. 6. Spike-like solution of equation $\partial^4 u(x) = 0$, with singularity capped at the molecular scale r_{UV}.

The distances of the spikes in these arrays are of the order of the length scale $r_{\text{m}} = 1/c_{\text{m}}$ supplied by the extrema in Figure 2.

The important point is now that there must be a preferred amplitude A of the spike-like solution (39), fixed by the interplay between r_{m} and the molecular size r_{UV} (as in the Monte-Carlo calculation in Ref. [8]). If this is the case, we can insert a superposition of these solutions into the energy (37) and find a partition function

$$\tilde{Z}_{\text{mem}} = \sum_{\{x_i, x_f\}} \exp \left[-\frac{\kappa_0}{2} A^2 \right.$$
$$\left. \times \int \mathrm{d}^2 x \int \mathrm{d}^2 x' \, n(x) G_4(x - x') n(x') \right], \tag{40}$$

Fig. 7. Pair of spikes, quadrupole, and multipole solutions of differential equation $\partial^4 u(x) = 0$, with singularities capped at the molecular scale r_{UV}.

where $n(x)$ is a sum of δ-functions at the positions of the spikes (with a minus sign for antispikes), and

$$
\begin{aligned}
G_4(x - x') &= \int \frac{\mathrm{d}^2 k}{(2\pi)^2} \frac{e^{ik(x-x')}}{k^4} \\
&= u_{\mathrm{sp2}}(x - x') + c_1(x - x')^2 + c_2 \qquad (41)
\end{aligned}
$$

is the correlation function of the field $u(x)$ containing two infinite constants from the infrared divergence of the integral. The infinity c_2 drops out for neutral spike-antispike systems with $\int \mathrm{d}^2 x\, n(x) = 0$. The infinity c_1 drops out under the condition of *dipole neutrality* $\int \mathrm{d}^2 x\, x\, n(x) = 0$. This follows directly by rewriting the interaction energy associated with c_1 as

$$
\begin{aligned}
&\int \mathrm{d}^2 x \int \mathrm{d}^2 x'\, n(x)\,(x - x')^2 n(x') \\
&= 2\int \mathrm{d}^2 x\, x^2\, n(x) \int \mathrm{d}^2 x'\, n(x') - 2\int \mathrm{d}^2 x\, x\, n(x) \int \mathrm{d}^2 x'\, x'\, n(x') \\
&= -2 \int \mathrm{d}^2 x\, x\, n(x) \int \mathrm{d}^2 x'\, x'\, n(x') = 0.
\end{aligned}
$$
$$(42)$$

Note that the purely logarithmic spike-like solutions of the wormhole type $u_{\mathrm{sp}}(x) = u_{\mathrm{wh}}(x)$ inFigure 4 do not have a long-range attraction between them.

The partition function (40) is obviously equivalent to the local one

$$
\begin{aligned}
\tilde{Z}_{\mathrm{mem}} = \sum_{\{x_i, x_f\}} \prod_x \left[\int \mathrm{d}u(x) \right] \exp \Big\{ \kappa_0 \\
\times \int \mathrm{d}^2 x \left[\frac{1}{2} [\partial^2 u(x)]^2 - A i u(x) n(x) \right] \Big\},
\end{aligned}
$$
$$(43)$$

or, in analogy with (36), to

$$
\begin{aligned}
\tilde{Z}_{\mathrm{mem}} \approx \prod_x \left[\int \mathrm{d}u(x) \right] \exp \Big\{ -\kappa_0 \\
\times \int \mathrm{d}^2 x \left[\frac{1}{2} [\partial^2 u(x)]^2 - \frac{z}{\kappa_0} \cos[A \kappa_0 u(x)] \right] \Big\}.
\end{aligned}
$$
$$(44)$$

This system is the dual transform of a two-dimensional crystal with defects whose phase properties have been thoroughly studied [20]. As it stands, the partition function (44) has a single first-order transition [21] from a spiky to a smooth surface. If the short-range properties of the model are slightly modified at a length scale l, the first-order transition splits into a sequence of two Kosterlitz-Thouless-like transitions, in which the spikes first form a gas of dipole pairs, and then a gas of quadrupoles [22] (see the figure in p. 1303 of Ref. [20]).

Upon further modifying the short-range properties, the quadrupoles may combine to a liquid of spikes and antispikes, which may be the structures seen in the experiments in Figure 1. The liquid could also freeze to a solid. Future experiments should look for quadrupoles and dipoles to confirm the correctness of these ideas.

It is essential that nonlinearities in the curvature energy fix an optimal size of the amplitude A in (40). For a purely quadratic surface energy (1), such an optimal A cannot exist since the energy of a spike-like solution (39) can be reduced continuously to zero by letting A go to zero.

5 Possible consequences for string theory

Such nonlinearities may also resolve an an old riddle in the string theory of *permanent quark confinement*. Quarks and antiquarks are held together at all distances by color-electric flux tubes formed from nonabelian gauge fields of quantum chromodynamics. In a Euclidean spacetime with $d = 4$, these tubes form fluctuating surfaces. In string theory, the behavior of such surfaces is investigated in an idealized form, considering them as infinitely thin objects possessing initially only surface tension (*Nambu-Goto strings*). But soon it was found that these surfaces would be unstable against the formation of infinitely thin protrusions, which do not possess any surface energy but a large configurational entropy (*plumber's nightmare*). This instability would ruin quark confinement. To avoid this, a curvature stiffness energy was added to the surface tension [23]. The resulting Euclidean *stiff-string* action was equal to the energy (7). However, this did not seem to lead to the desired stabilization since, in an infinite number of dimensions, there exists a finite persistence length beyond which quark would no longer be confined. It remained unclear whether this phenomenon would persist down to $d = 4$. The present discussion gives rise to the hope that the persistence length can become infinite after all. Since $d = 4$ in (7) corresponds to $N = 2$ in the nonlinear σ-model (22), which possesses a smooth phase with long-range correlations, the λ-fluctuations in the action (9) may be violent enough to produce so many zeros in $\lambda(x)$ that $\langle \lambda(x) \rangle = 0$ and the persistence length in infinite, implying permanent quark confinement. But we also have learned that this may occur only with support from higher nonlinear terms in the curvature energy. A color-electric flux tube certainly has such additional terms, although it differs from the membranes discussed in this paper in an important point: Its curvature stiffness is negative, as was recently shown by the author and Chevyakov [24].

All papers by the author quoted in the list of references can be read on the world wide web at http://www.physik.fu-berlin.de/~kleinert/kleiner_re0.html.

References

1. M.M. Kozlov, W. Helfrich, J. Phys. II France **4**, 1427 (1994); Phys. Rev. E **51**, 3324 (1995); B. Fourcade, Ling Miao, M. Rao, M. Wortis, R.K.P. Zia, Phys. Rev. E **49**, 5276 (1994); U. Seifert, J. Shillcock, P. Nelson, Phys. Rev. Lett. **77**, 5237 (1996); T. Charitat, B. Fourcade, J. Phys. II France **7**, 15 (1997).

2. J.B. Fournier, Phys. Rev. Lett. **76**, 4436 (1996).

3. T. Fisher, J. Phys. II France **2**, 337 (1992); **3**, 1795 (1993); H. Kleinert, Phys. Lett. B **211**, 151 (1988); Phys. Lett. A **136**, 253 (1989).

4. B. Klösgen, W. Helfrich, Eur. Biophys. J. **22**, 329 (1993); Biophys. J. **73**, 3016 (1997).

5. H.J. Deuling, W. Helfrich, J. Phys. France **37**, 1335 (1976); W. Harbich, H.J. Deuling, W. Helfrich, J. Phys. France **38**, 727 (1976).

6. P.B. Canham, J. Theor. Biol. **26**, 61 (1970); W. Helfrich, Z. Naturforsch. B **103**, 167 (1975).

7. M. Kiometzis, H. Kleinert, Phys. Lett. A **140**, 520 (1989).

8. R. Goetz, W. Helfrich, J. Phys. II France **6**, 215 (1996).

9. L. Peliti, S. Leibler, Phys. Rev. Lett. **54**, 1690 (1985).

10. H. Kleinert, Phys. Lett. A **114**, 263 (1985).

11. P.-G. de Gennes, C. Taupin, J. Phys. Chem. **86**, 2294 (1982).

12. G. Gompper, D.M. Kroll, Europhys. Lett. **19**, 581 (1992); Science **255**, 968 (1992).

13. H. Kleinert, Phys. Lett. A **116**, 57 (1986); H. Kleinert, S. Ami, Phys. Lett. A **120**, 207 (1987); H. Kleinert, J. Stat. Phys. **56**, 227 (1989); B.D. Simons, M.E. Cates, J. Phys. II France **2**, 1439 (1992); D.C. Morse, S.T. Milner, Europhys. Lett. **26**, 565 (1994).

14. A. Polyakov, Nucl. Phys. B **268**, 406 (1986); H. Kleinert, Phys. Lett. B **174**, 335 (1986); Phys. Rev. Lett. **58**, 1915 (1987); Phys. Lett. B **189**, 187 (1987); Phys. Rev. D **40**, 473 (1989).

15. T.H. Berlin, M. Kac, Phys. Rev. **86**, 82 (1952).

16. For a detailed review see Section 11.13 in Vol. I of the textbook H. Kleinert, *Gauge Fields in Condensed Matter*, Vol. I: *Superflow and Vortex Lines*, pp. 1–744, Vol. II: *Stresses and Defects*, pp. 744-1443 (World Scientific, Singapore, 1989).

17. For the wide use of these generalized δ-functions in many fields of physics see the textbook in [16], and the Cambridge lectures: H. Kleinert, "Theory of Fluctuating Non-holonomic Fields and Applications: Statistical Mechanics of Vortices and Defects, and New Physical Laws in Spaces with Curvature and Torsion", in *Proceedings of a NATO Advanced Study Institute* on Formation and Interactions of Topological Defects at the University of Cambridge, England, 1996 (`cond-mat/9503030`).

18. See Section 11.15 in Vol. I of the textbook in [17].

19. See equation (11A.60) in Vol. II of the textbook in [17].

20. See Chapter 14 of Vol. II in the textbook in [17].

21. H. Kleinert, Phys. Lett. A **95**, 381 (1983); W. Janke, H. Kleinert, Phys. Lett. A **105**, 134 (1984); Phys. Lett. A **114**, 255 (1986).

22. H. Kleinert, Phys. Lett. A **130**, 443 (1988); Phys. Lett. A **136**, 468 (1989); W. Janke, H. Kleinert, Phys. Rev. Lett. **61**, 2344 (1988); Phys. Rev. A **41**, 6848 (1990).

23. A. Polyakov, A.M. Polyakov, Nucl. Phys. B **268**, 406 (1986); H. Kleinert, Phys. Lett. B **174**, 335 (1986).

24. H. Kleinert, A. Chervyakov, Phys. Lett. B **381**, 286 (1996) (`hep-th/9601030`).